Mass imbalance and electron-phonon correlation impact on the excitonic insulator state in semimetal/semiconducting materials

Thi-Hong-Hai Do [1], Thi-Hau Nguyen [1,2] and Van-Nham Phan [3,4,*]

[1] *Department of Physics, Hanoi University of Mining and Geology, Duc Thang, Bac Tu Liem, Hanoi 10072, Vietnam*

[2] *Faculty of Physics, Graduate University of Science and Technology, Vietnam Academy of Science and Technology, Hanoi 10072, Vietnam*

[3] *Institute of Research and Development, Duy Tan University, 3-Quang Trung, Danang 550000, Vietnam*

[4] *Faculty of Natural Sciences, Duy Tan University, 3-Quang Trung, Danang 550000, Vietnam*

(Received 29 November 2023; revised 15 January 2024; accepted 17 January 2024; published 5 February 2024)

Signatures of the excitonic insulator in the mass-imbalance extended Falicov-Kimball model with the electron-phonon correlation are investigated. Based on the unrestricted Hartree-Fock approximation, we derive a set of self-consistent equations specifying the excitonic insulator order parameter and then construct the complex phase diagram of the excitonic insulator states. For a given intermediate Coulomb interaction, the excitonic insulator states at nearly zero temperature are found if the electronic hybridization-phonon coupling is sufficiently large. The window of the excitonic insulator states expands as suppression of the mass anisotropy. The influence of the mass imbalance and electron-phonon correlations on the nature of the BCS-BEC crossover of the condensation states is also addressed in the signatures of the optical conductivity. The preformed excitonic bound states in the normal semiconducting side are inspected in the features of the imaginary part of the dynamical excitonic susceptibility function. By increasing the electronic hybridization-phonon coupling or suppressing the mass imbalance, we find the dominance of the excitonic coherent bound states. The compact influence of the mass imbalance and electron-phonon correlations on the whole picture of the excitonic insulator state thus has been discussed.

DOI: 10.1103/PhysRevB.109.085105

I. INTRODUCTION

The condensation state of bosonic quasiparticles is always one of the most interesting subjects in many-particle physics [1,2]. In a semiconductor (SC) or a semimetal (SM), due to the Coulomb attraction, the conduction band electrons and the valence band holes may couple to each other to form a bosonic quasiparticle so-called exciton. At sufficiently low temperatures, a large number of the excitons might spontaneously condense into a single quantum coherent state as proposed by the Bose-Einstein condensation (BEC) theory. Unlike the Cooper pairs in superconductivity, excitons are neutral quasiparticles so the excitonic condensation state is an insulator and that condensate is termed as an excitonic insulator (EI) state. The EI state in a material was proposed theoretically since the early 1960s [3–5] and, recently, the field of studying the EI state has been focused due to its observations in experiments [6–11]. In the experimental observations, one has been released that the Coulomb interaction is not a pure partner mediating the coupling between the conduction electrons and valence holes. In that situation, the electron-phonon correlations also significantly impact on the stability of the EI state [6–11]. The separation which interaction is relevant in driving the EI state is indeed impossible [11]. On the theoretical side, the excitonic condensation state driven by both Coulomb interaction and electron-phonon correlations has been intentively studied [11–16]. In these studies, the Coulomb interaction is considered in the Falicov-Kimball form so the electronic model describing the EI state in the system is called the extended Falicov-Kimball model (EFKM) in which the valence hole band is not completely localized as in the original version [17]. In the framework of the pure EFKM, depending on the Coulomb attraction, the EI state has been described likely either as superconductivity in the theory of Bardeen–Cooper–Schrieffer (BCS) or the BEC of preformed excitons. The BCS-BEC crossover of the EI state has been then addressed and exhibits many interesting phenomena [18,19].

In the EFKM, the valence electrons are assumed to be flexible, i.e., they can hop between the lattice sites and their effective mass is finite. The EFKM is thus able to describe in more realistic the excitonic condensation states in the semimetal-semiconducting transition materials [20,21]. In these materials, the valence holes are heavier than the conduction electrons and the hopping amplitude between nearest neighbors of the valence holes $|t^f|$ is smaller than that of the conduction electrons $|t^c|$ [12–16,18,19]. In the other systems such as the double layer structures fabricated by graphene or quantum wells, the general features of the EFKM can also be utilized in investigating the interlayer hybridizations [22–24]. In such systems, the effective mass of the conduction and valence electrons are almost equal [25]. These evidents release that the EFKM has opened a widely ranged application in inspecting the physical signatures in the semimetal/semiconducting systems by varying the difference

*Corresponding author: phanvannham@duytan.edu.vn

between the hopping amplitudes or the mass imbalance of the conduction and valence electrons [26]. Investigating the mass imbalance in the EFKM impacting on the excitonic instability thus is an essential issue. However, as addressed above, the EFKM alone is a purely electronic model that is thus inconsistent with some experimental observations in real materials, for instance, in the transition metal dichalcogenides Ta_2NiSe_5 in which the electronphonon correlations play important roles in the formation of the excitonic condensation state [8–10,27,28]. Inspecting the impression of the electron-phonon correlations and also the mass imbalance thus is an important issue in undertanding the nature of the EI instability in the semimetal/semiconducting materials, in general.

In the present work, the influence of the mass imbalance and electron-phonon correlations on the EI state is examined in the framework of the EFKM involving the electronic hybridization-phonon coupling. By utilizing the unrestricted HartreeFock (UHF) approximation, we can find a set of self-consistent equations determining the EI order parameters when both the electron-phonon and the Coulomb interactions are treated on an equal footing. In the UHF approximation, all fluctuations are suppressed. However, in low and especially in the zero-temperature limitations, the UHF approximation has verified itself as an applicable method applying even for some strongly correlated electron systems by comparing with other more effective methods such as the dynamical mean-field theory—one of the best theoretical approaches sucessfully applied to the strongly correlated electron systems [29,30], the unbiased constrained path Monte Carlo simulation [31,32], or the density matrix renormalization group [33,34]. In the present work, by adapting the UHF approximation we construct the ground-state phase diagram of the EI state and also its BCS-BEC crossover by analyzing the momentum distribution of the EI order parameters. In the Kubo linear response theory, we estimate the real part of the optical conductivity. Signatures of the EI state in both BCS and BEC types in the presence of external optical excitation are addressed. In the normal semiconducting state, we also evaluate the dynamical excitonic susceptibility function. By increasing the electron-phonon correlations or suppressing the mass imbalance, its imaginary part releases the resonance signatures indicating the excitonic coherent bound state even in the semiconducting state. That is evidence of the "halo" phase specifying the preformed excitons existing outside the EI state.

This paper is organized as follows. In Sec. II, we present the Hamiltonian of the EFKM including electronic hybridization-phonon coupling written in the momentum space. The analytical calculations specifying the set of self-consistent equations evaluating the EI order parameters are outlined. The numerical results and discussion are addressed in Sec. III. The last section summarizes our present work.

II. MODEL AND THEORETICAL CALCULATION

To inspect the impact of the mass imbalance and electron-phonon correlations on the instability of the excitonic insulator state in semimetal semiconductor transition materials, in our work, we use the spinless EFKM involving the electron-phonon correlation that is described below by the

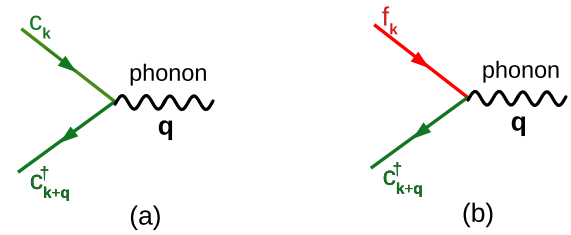

FIG. 1. Sketched Feynman diagrams of the common electronic hybridization-phonon coupling (a) and the conduction-valence electronic hybridization-phonon interaction (b).

Hamiltonian written in the momentum space,

$$\mathcal{H} = \sum_{\mathbf{k}} \left(\varepsilon^c_{\mathbf{k}} c^\dagger_{\mathbf{k}} c_{\mathbf{k}} + \varepsilon^f_{\mathbf{k}} f^\dagger_{\mathbf{k}} f_{\mathbf{k}}\right) + \frac{U}{N} \sum_{\mathbf{k}\mathbf{k}'\mathbf{q}} c^\dagger_{\mathbf{k}+q} c_{\mathbf{k}} f^\dagger_{\mathbf{k}'-\mathbf{q}} f_{\mathbf{k}'} + \sum_{\mathbf{k}} \omega_0 p^\dagger_{\mathbf{k}} p_{\mathbf{k}} + \frac{g}{\sqrt{N}} \sum_{\mathbf{k}\mathbf{q}} [c^\dagger_{\mathbf{k}+\mathbf{q}} f_{\mathbf{k}} (p^\dagger_{-\mathbf{q}} + p_{\mathbf{q}}) + \text{H.c.}], \tag{1}$$

where $c^{(\dagger)}_{\mathbf{k}}$, $f^{(\dagger)}_{\mathbf{k}}$, and $p^{(\dagger)}_{\mathbf{k}}$ are respectively the annihilation (creation) operators of the spinless conduction, valence electrons, and the phonons with the momentum $\mathbf{k}$. The first two terms in Eq. (1) express the kinetic energy of the conduction and valence electrons with respect to their dispersion relations $\varepsilon^c_{\mathbf{k}}$ and $\varepsilon^f_{\mathbf{k}}$. In the tight-binding approximation, the dispersion relations read

$$\varepsilon^{c/f}_{\mathbf{k}} = \varepsilon^{c/f} - 2t^{c/f}\gamma_{\mathbf{k}} - \mu. \tag{2}$$

Here $t^{c/f}$ is the hopping integral of the c/f electron with its onsite energy $\varepsilon^{c/f}$, $\gamma_{\mathbf{k}} \equiv \cos k_x + \cos k_y$ for a two-dimensional hypercubic lattice, and μ is the chemical potential. The amplitude of the hopping integral $t^{c/f}$ is inversely dependent on the effective mass of the c/f electron. The difference between t^c and t^f thus delivers the mass imbalance of the electron-hole system. The second term in Eq. (1) describes the localized Coulomb interaction or the Falicov-Kimball interaction between the conduction and valence electrons written in the momentum space. The first line in Eq. (1) thus is the Hamiltonian of the EFKM [26,35,36]. Its mass-imbalance effects on the EI instability in the semimetal-semiconducting transition materials have been recently discussed [26]. The second line in Eq. (1) specifies a phononic correlation with the electrons in the system. The phonon here is assumed dispersionless being described by the Einstein model with a constant energy ω_0. The coupling between the electronic system and phonons is expressed in the last term in Eq. (1). Both U and g in Eq. (1) thus release the strengths of the Coulomb interaction and the conduction-valence electronic hybridization-phonon coupling, respectively, expressing the correlations in the electronic-phononic system. Note that the electronic hybridization-phonon coupling here is different to the common electron-phonon coupling as in the literatures. Indeed, the common electron-phonon interaction considers the process of the annihilation and creation of an electron on the same band with respect to the absorption or emission of phonons [Fig. 1(a)]. In the meanwhile, the electronic hybridization-phonon coupling specifies the process of the

annihilation of an electron (or the creation of a hole) on the valence band and the creation of the electron on the conduction band with the absorption or emission of phonons [Fig. 1(b)]. The exciting electron-hole pair with phonon interaction here can be considered as the excitation of exciton mediated by the lattice displacement [37]. In general, the other potentials such as the common electron-phonon coupling or the Coulomb repulsions between electrons on the same band should be involved. However, these interactions do not directly affect on the excitonic condensate signatures and they are left in the present study.

The Hamiltonian written in Eq. (1) is a complex model formulating the many-body problems. It probably could not be solved exactly and one has to find some approximations. In our present work, we use the UHF approach to solve the Hamiltonian by ignoring all its fluctuation parts. By depleting all fluctuations, the UHF approximation generally is considered as a crude approach. However, in low or especially in the zero-temperature limitations, the UHF approximation surprisingly releases the equivalent solutions to other more effective methods such as the dynamical mean-field theory—one of the best theoretical approaches successfully applied to the strongly correlated electron systems [29,30], the unbiased constrained path Monte Carlo simulation [31,32], or the density matrix renormalization group [33,34]. That reason stimulates us to utilize the UHF approach in solving the Hamiltonian written in Eq. (1), its effective Hamiltonian reads

$$\mathcal{H}_{\rm UHF} = \sum_{\mathbf{k}} \left(\bar{\varepsilon}^c_{\mathbf{k}} c^\dagger_{\mathbf{k}} c_{\mathbf{k}} + \bar{\varepsilon}^f_{\mathbf{k}} f^\dagger_{\mathbf{k}} f_{\mathbf{k}}\right) + \delta \sum_{\mathbf{k}} (c^\dagger_{\mathbf{k}} f_{\mathbf{k}} + \text{H.c.}) + \sum_{\mathbf{q}} \omega_0 p^\dagger_{\mathbf{q}} p_{\mathbf{q}} + \sqrt{N}\eta (p^\dagger_{-\mathbf{q}} + p_{\mathbf{q}})\delta_{\mathbf{q},\mathbf{0}}. \tag{3}$$

Here the dispersion relations of the conduction and valence electrons have been renormalized by the contribution of the Coulomb interaction in the UHF approach that are given by

$$\bar{\varepsilon}^{c/f}_{\mathbf{k}} = \varepsilon^{c/f}_{\mathbf{k}} + U n^{f/c}, \tag{4}$$

where $n^c = \sum_{\mathbf{k}} \langle c^\dagger_{\mathbf{k}} c_{\mathbf{k}}\rangle/N$ and $n^f = \sum_{\mathbf{k}} \langle f^\dagger_{\mathbf{k}} f_{\mathbf{k}}\rangle/N$ are respectively the conduction and valence electronic densities. $Un^{c/f}$ in Eq. (4) so can be called the Hartree shifts due to the contribution of the Coulomb interaction. In Eq. (3) δ and η are the additional fields that read

$$\eta = \frac{g}{N} \sum_{\mathbf{k}} \langle c^\dagger_{\mathbf{k}} f_{\mathbf{k}} + f^\dagger_{\mathbf{k}} c_{\mathbf{k}}\rangle, \tag{5}$$

$$\delta = \frac{g}{\sqrt{N}} \langle p^\dagger_{-\mathbf{q}} + p_{\mathbf{q}}\rangle \delta_{\mathbf{q},\mathbf{0}} - \frac{U}{N} \sum_{\mathbf{k}} \langle c^\dagger_{\mathbf{k}} f_{\mathbf{k}}\rangle, \tag{6}$$

and play the role of the EI order parameters. In that manner, the nonzero of these order parameters indicates the stability of the excitonic condensate in the system. Note here that, in our situation, we have assumed the system as the direct semiconductors, i.e., the top of the valence band and the bottom of the conduction band are located at the center of the Brillouin zone. The bound state should be promoted mainly by coupling between the conduction and valence electrons with the same momentum. In that situation, only zero-momentum phonons contribute to mediate the excitonic bound states.

The effective Hamiltonian written in Eq. (3) can be simply diagonalized by using the Bogoliubov transformation. Defining new fermionic operators in the forms

$$\varphi^\dagger_{\mathbf{k}} = u_{\mathbf{k}} c^\dagger_{\mathbf{k}} + v_{\mathbf{k}} f^\dagger_{\mathbf{k}}, \tag{7}$$

$$\psi^\dagger_{\mathbf{k}} = -v_{\mathbf{k}} c^\dagger_{\mathbf{k}} + u_{\mathbf{k}} f^\dagger_{\mathbf{k}}, \tag{8}$$

with $u_{\mathbf{k}}$ and $v_{\mathbf{k}}$ are chosen such that $u^2_{\mathbf{k}} + v^2_{\mathbf{k}} = 1$, the electronic part [the first line in Eq. (3)] of the effective Hamiltonian can be diagonalized as

$$\mathcal{H}^e_{\rm dia} = \sum_{\mathbf{k}} (E^+_{\mathbf{k}} \varphi^\dagger_{\mathbf{k}} \varphi_{\mathbf{k}} + E^-_{\mathbf{k}} \psi^\dagger_{\mathbf{k}} \psi_{\mathbf{k}}), \tag{9}$$

where the Bogoliubov fermionic quasiparticle energies are given by

$$E^\pm_{\mathbf{k}} = \frac{\bar{\varepsilon}^f_{\mathbf{k}} + \bar{\varepsilon}^c_{\mathbf{k}}}{2} \mp \frac{\text{sgn}(\bar{\varepsilon}^f_{\mathbf{k}} - \bar{\varepsilon}^c_{\mathbf{k}})}{2} \Gamma_{\mathbf{k}}, \tag{10}$$

with

$$\Gamma_{\mathbf{k}} = \sqrt{\left(\bar{\varepsilon}^c_{\mathbf{k}} - \bar{\varepsilon}^f_{\mathbf{k}}\right)^2 + 4|\delta|^2}. \tag{11}$$

The phononic part [the second line in Eq. (3)] can also be diagonalized by defining a new phonon operator,

$$P^\dagger_{\mathbf{q}} = p^\dagger_{\mathbf{q}} + \sqrt{N}\frac{\eta}{\omega_0}, \tag{12}$$

and one finds

$$\mathcal{H}^{\rm ph}_{\rm dia} = \sum_{\mathbf{q}} \omega_0 P^\dagger_{\mathbf{q}} P_{\mathbf{q}}. \tag{13}$$

From the diagonal form of the electronic part in Eq. (9), we can evaluate the the expectation values to close the set of self-consistent equations, such as

$$n^c = \frac{1}{N} \sum_{\mathbf{k}} \left[u^2_{\mathbf{k}} f(E^+_{\mathbf{k}}) + v^2_{\mathbf{k}} f(E^-_{\mathbf{k}})\right],$$

$$n^f = \frac{1}{N} \sum_{\mathbf{k}} \left[v^2_{\mathbf{k}} f(E^+_{\mathbf{k}}) + u^2_{\mathbf{k}} f(E^-_{\mathbf{k}})\right],$$

$$\eta = -\frac{2g\delta}{N} \sum_{\mathbf{k}} \frac{\text{sgn}(\bar{\varepsilon}^c_{\mathbf{k}} - \bar{\varepsilon}^f_{\mathbf{k}})}{\Gamma_{\mathbf{k}}} [f(E^+_{\mathbf{k}}) - f(E^-_{\mathbf{k}})], \tag{14}$$

where $f(E^\pm_{\mathbf{k}}) = 1/[1 + e^{\beta E^\pm_{\mathbf{k}}}]$ is the Fermi-Dirac distribution function with $\beta = 1/T$ and T is the temperature.

The diagonalized form of the phononic part delivered in Eq. (13) permits us to evaluate the rest expectation value in Eq. (6); it reads

$$\langle p^\dagger_{-\mathbf{q}} + p_{\mathbf{q}}\rangle \delta_{\mathbf{q},\mathbf{0}} = -2\frac{\sqrt{N}h}{\omega_0}. \tag{15}$$

From the expressions in Eqs. (4)–(6), (14), and (15), we find a set of self-consistent equations that can be solved by numerical methods to evaluate the expectation values and renormalized quasiparticle energies.

III. NUMERICAL RESULTS AND DISCUSSION

In this section, we present the numerical results discussing the effects of the mass imbalance and the electronic

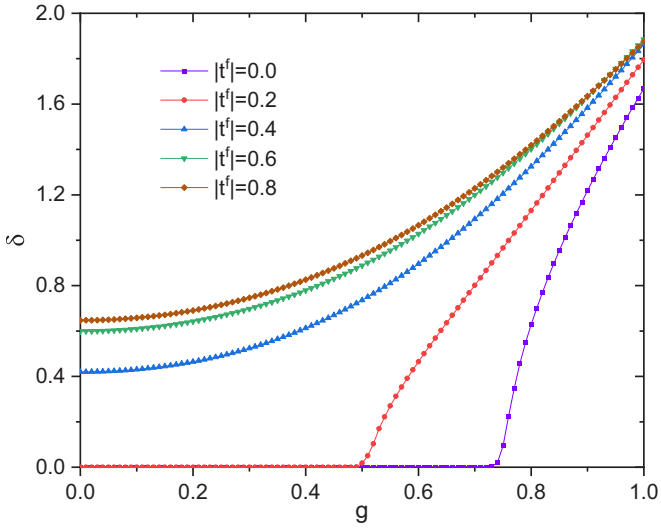

FIG. 2. EI order parameter δ as a function of the electronic hybridization-phonon coupling g for different hopping amplitudes of the valence electrons $|t^f|$ at $U = 3.5$.

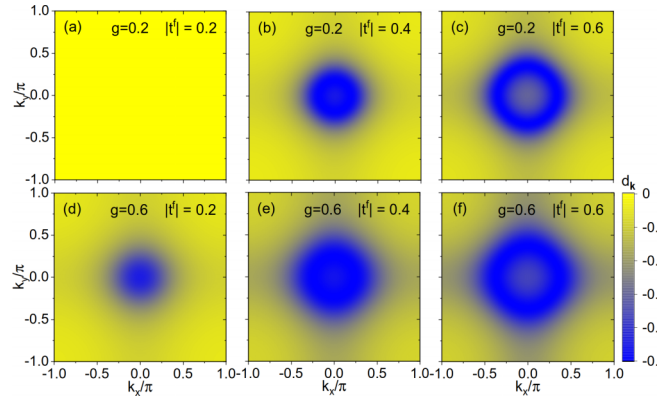

FIG. 3. Magnitude of the EI order parameter $d_{\mathbf{k}}$ depending on momentum $\mathbf{k}$ in the first Brillouin zone in the ground state for different values of $|t^f|$ with $g = 0.2$ (top) and $g = 0.6$ (bottom) at $U = 3.5$.

hybridization-phonon coupling on the properties of the EI state in the EFKM at very low temperature $T \approx 0$. The self-consistent Eqs. (4)–(6), (14), and (15) are solved numerically for the two-dimensional square lattice with $N = 500 \times 500$ lattice sites. In the numerical calculation, we set $t^c = 1$ as the unit of energy and fix the separation between the c and the f bands as $\varepsilon^c - \varepsilon^f = 2.0$. In this situation, the two noninteracting bands are overlapped and the system settles in the semimetallic side. The chemical potential μ in the Hamiltonian or in Eq. (4) is adjusted to specify the half-filling band case, i.e., the total electronic density: $n^c + n^f = 1$. In the previous studies, we have confirmed that the physical scenario in both the adiabatic limit and the antiadiabatic limit is not significantly different [14,15,38]. In this paper, the phonon frequency $\omega_0 = 2.0$, therefore, is chosen as a special case of the antiadiabatic situation.

In order to address the impacts of the mass imbalance and electron-phonon correlations on the EI state, we first present in Fig. 2 the dependence of the EI order parameter δ [evaluated in Eq. (6)] on the electronic hybridization-phonon coupling with different hopping amplitudes of the valence electrons $|t^f|$ at an intermediate Coulomb interaction $U = 3.5$. At $|t^f| = 0$, i.e., when the valence band is flat or the mass of the valence electrons is infinite, the EI does not exist if there is no electron-phonon correlation, because of the Elitzur's theorem [39]. Indeed, in the limited cases, the Hamiltonian given in Eq. (1) recovers the original Falicov-Kimball model (FKM) [17] it, therefore, possesses a local $U(1)$ symmetry related to the localized valence electrons. Following the Elitzur theorem, there should be no spontaneous hybridization between the valence and conduction electrons [40]. The EI in the situation is found only if the electronic hybridization-phonon coupling is sufficiently large that impresses the significant role of the electron-phonon correlations in establishing and stabilizing the EI state in the systems. This signature is unchanged if the effective mass of valence electron is finite but still large or its hopping term is lightly increased, for instance up to $|t^f| = 0.2$. However, the scenario is completely changed if the hopping term of the valence electrons is further increased. Indeed, at $|t^f| \geqslant 0.4$, one finds the stability of the EI state even without the electronic hybridization-phonon coupling. The Coulomb interaction only in this situation is sufficient to form and stabilize the excitonic condensation state. Enlarging the electronic hybridization-phonon coupling plays the role of reinforcing the stability of the EI state. The difference of $|t^f|$ and $|t^c|$ or the masses between the valence and conduction electrons thus significantly affects the stability of the excitonic condensation state. Indeed, in case of large mass difference, the valence electrons would be much more localized than conduction partners, the conduction and valence electrons thus are hard to hybridize, and one finds the difficulty in the formation of the excitonic coherent state. The hybridization is reinforced once the mass of the valence electrons becomes comparable with that of the conduction electrons. The valence electrons in this condition would be more flexible and, as a consequence, the excitonic coherent state can be established at small or even without the electronic hybridization-phonon coupling.

To inspect the nature of the excitonic condensation states, we show in Fig. 3 the momentum dependence of the EI order parameter $d_{\mathbf{k}} = \langle c^\dagger_{\mathbf{k}} f_{\mathbf{k}} \rangle$ by varying the hopping term of the valence electrons $|t^f|$ and the electronic hybridization-phonon coupling g for a given intermediate Coulomb interaction $U = 3.5$. Our results release that at a given low electronic hybridization-phonon coupling, the EI stability is found only if the mass of valence electrons becomes comparable with that of the conduction electrons. Indeed, Fig. 3 shows us that signature of the $d_{\mathbf{k}}$ is only visible if $|t^f| \geqslant 0.2$ [see Fig. 3(b) and 3(c)]. Inspecting profoundly the signature of the momentum dependence of the EI order parameter one finds that at low $|t^f|$, for instance at $|t^f| = 0.2$, $d_{\mathbf{k}}$ shows a sharp peak at zero momentum, indicating the BEC type of the excitonic condensation state. In this case, the Hartree shift due to the presence of Coulomb interaction has moved the system to the semiconducting situation. With a large mass imbalance of the conduction and valence electrons, the less flexible valence electrons make a separation between the conduction and

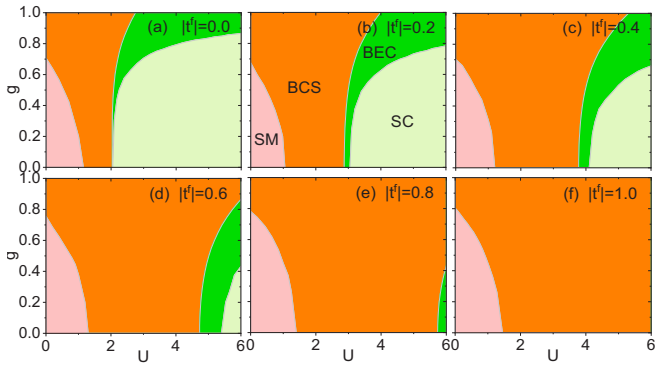

FIG. 4. The phase diagram of the EI in the (U, g) plane for different values of the valence transfer integral $|t^f|$. The EI state being in BCS type and BEC type are indicated by the orange and green region, while the SM and SC state are pointed out by the pink and yellow region, respectively.

valence bands. The excitonic bound-state formation in this situation is strong like a natural atom and as a consequence, they might condense following the BEC theory. That feature is completely changed in case of a smaller mass imbalance. Indeed, in case of increasing $|t^f|$ for instance up to $|t^f| = 0.4$, one finds the outspread of the $d_{\mathbf{k}}$; however, it gets maximum at finite momentum. In this situation, due to the lowering mass of the valence electrons, the two conduction and valence bands overlap each other and thus the Fermi level plays an important role in establishing the formation of the excitonic bound state. That scenario looks like the feature proposed by the BCS theory explaining the coherent bound state of the Cooper pairs in the superconducting theory. The excitons in this case thus might condense to form the EI state in the so-called BCS type. By increasing the electronic hybridization-phonon coupling, the BCS-BEC crossover signature of the EI state is unaltered, except that it might happen at the smaller mass imbalance of the conduction and valence electrons (see low panels of Fig. 3). Moreover, with the help of the strengthened electron-phonon correlations, the large mass valence electrons are able to get a coupling to the conduction ones establishing the excitonic bound state.

To summarize the effect of the mass imbalance in the presence of both the electronic hybridization-phonon coupling and the Coulomb interaction on the stability of the EI in the ground state we show in Fig. 4 the phase diagram in (U, g) plane for different values of $|t^f|$. The boundary of the EI instability is established from the EI order parameter at which it becomes neglectable. The critical can be also evaluated by the divergence of the static excitonic susceptibility function. Both these results are equilvalent [38]. The BCS-BEC crossover of the EI stability is released in the signature of the momentum distribution of the EI order parameter $d_{\mathbf{k}}$ as addressed in Fig. 3. The SC or SM states are specified through the renormalized band structure [19,41]. The phase diagram shows us that at a given set of small electronic hybridization-phonon coupling and large mass imbalance one always finds a window of the EI stability settled between two critical values of the Coulomb interaction U_{c1} and U_{c2}. At a given mass imbalance, i.e., for fixed $|t^f|$, by increasing the electron-phonon correlations, the EI window is expanded. The EI stability even can be found without of the Coulomb interaction if the electronic hybridization-phonon coupling is sufficiently large. In that case, the large electron-phonon correlations alone can establish the stability of the coherent bound state of the excitons in the system. At a small Coulomb interaction, one finds the SM-EI in BCS type transition, in the meanwhile, in a large Coulomb interaction range, the SC-EI in BEC type transition is addressed by increasing the electronic hybridization-phonon coupling. Reinforcing the electron-phonon correlations in one way enlarges the EI state, the other way it expands rapidly the BEC-EI stability at an intermediate value specifying the significant roles of the electron-phonon correlations in establishing the stability of the EI state. From Figs. 4(a)–4(f), we find that as lowering the mass imbalance between the conduction and the valence electrons, the EI stability window also expands in the same arrangements of the electronic hybridization-phonon coupling and the Coulomb interaction. Lowering the mass imbalance apparently raises the hybridization possibility between the valence and the conduction electrons. In that sense, it promotes the stability of the EI in the BCS type. At $|t^f| = 0$, i.e., the valence band is completely localized, we find that the BEC-EI state in the original FKM cannot be established without the sufficiently large electron-phonon correlation [cf. Fig. 4(a)]. However, that scheme is significantly changed in the case of finite valence bandwidth, especially, once the mass of valence electrons and its of conduction ones becomes comparable, when we find the BEC-EI stability even at zero electronic hybridization-phonon coupling (see the left panels of Fig. 4). That scenario once more specifies the important role of the mass imbalance in establishing the phase structure of the EI state in the system.

In order to describe in more detail the signatures of the EI states in the influence of the mass anisotropy and the electron-phonon correlations we address, hereafter, the dynamical properties of the system at the given intermediate Coulomb interaction $U = 3.5$. To do this, we first examine the real part of the optical conductivity $\sigma(\omega)$ that might be evaluated in the framework of the Kubo linear response theory [42]. In that manner, one finds

$$\sigma(\omega) = \frac{\pi e^2}{\omega N} \sum_{\mathbf{k}} u_{\mathbf{k}}^2 v_{\mathbf{k}}^2 \left(\nabla \varepsilon_{\mathbf{k}}^c - \nabla \varepsilon_{\mathbf{k}}^f\right)^2 [f(E_{\mathbf{k}}^+) - f(E_{\mathbf{k}}^-)] \times [\delta(\omega + E_{\mathbf{k}}^+ - E_{\mathbf{k}}^-) - \delta(\omega - E_{\mathbf{k}}^+ + E_{\mathbf{k}}^-)], \quad (16)$$

where $\nabla \varepsilon_{\mathbf{k}}^{c/f}$ is the grad of the dispersion relation of original noninteracting c/f electron that delivers the role of the velocity of the noninteracting conduction/valence electrons in the system [16,26,43]. With the solution of the self-consistent equations above, one can easily evaluate the real part of the optical conductivity in Eq. (16).

In Fig. 5 we show the real part of the optical conductivity $\sigma(\omega)$ at $|t^f| = 0.2$ for different electronic hybridization-phonon couplings g. For all g values, one always finds a single-peak structure at frequency $\omega_c = 2\delta$ of the optical conductivity spectrum. The peak indicates the resonance state due to the hybridization of the electron in the conduction band and the hole in the valence band corresponding to the

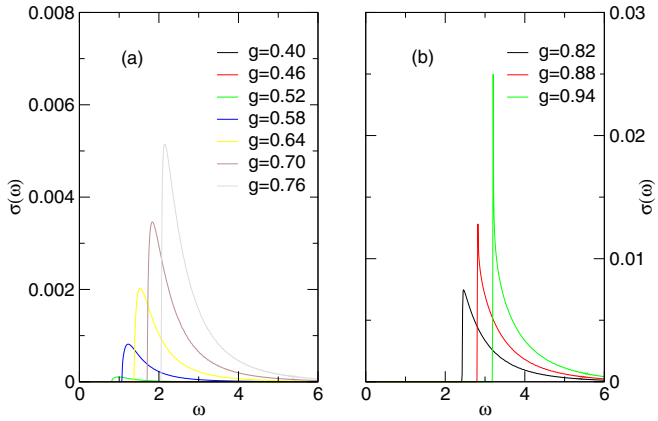

FIG. 5. The real part of the optical conductivity $\sigma(\omega)$ for different values of the electronic hybridization-phonon coupling g at $|t^f| = 0.2$ and $U = 3.5$.

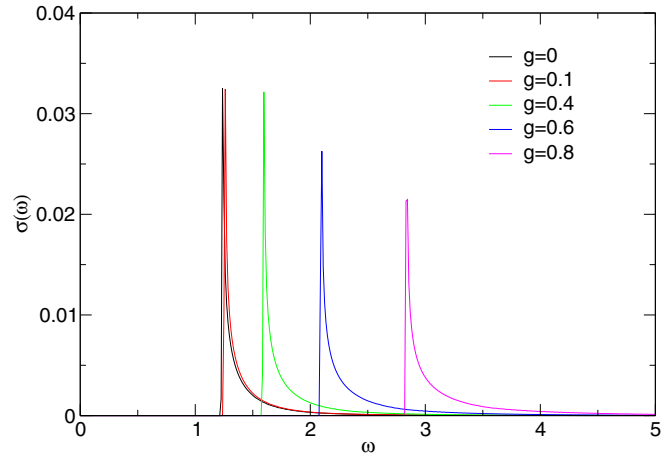

FIG. 6. The real part of the optical conductivity $\sigma(\omega)$ for different values of the electronic hybridization-phonon coupling g at $|t^f| = 0.6$ and $U = 3.5$.

boundary of the excitonic coherent state. Below ω_c, the optical conductivity is significantly suppressed due to the absence of available electronic states for absorption. That signature of the optical conductivity signifies the energy gap with respect to the stability of the excitonic condensation. Above the resonance frequency ω_c, the optical conductivity exhibits the Drude form releasing the normally excited quasiparticles settling above the excitonic condensation gap. The position and height of the Drude peak structure significantly change by varying the electronic hybridization-phonon coupling. Indeed, as increasing the electronic hybridization-phonon coupling, initially, one finds a gradual increase in the height with moving to the higher energy of the Drude peak. The moving to the higher energy of the Drude peak specifies the increasing of the EI order parameter while increasing its height releases a development of the electronic excited probability contributing to the formation of the bound excitonic condensate. Signatures of the optical conductivity spectra have thus specified the significant impact of the electronic hybridization-phonon coupling in the stability of the EI state as addressed in the phase diagram in Fig. 4. The low and blunter peak in the left panel of Fig. 5 specifies a low probability of excited electronic states and weak absorption light of the electronic excited states. In that situation, only some excited states around the center of the Brillouin zone contribute to the optical transitions. That signatures indicate the semiconducting state with the strongly bound state of the electron and hole, or the system stabilizes in the BEC type of the EI state. Increasing further the electronic hybridization-phonon coupling to $g > 0.6$, the right panel of Fig. 5 shows us that the Drude peak continuously shifts to the right. Its spectral weight rapidly increases with much more sharper at energy $\omega = \omega_c$. The sudden increase of the spectral weight indicates the high probability of the excited electronic states contributing to the optical transitions. In that situation, the sufficiently large electronic hybridization-phonon coupling has driven the system to the semimetal state with the overlap of the bared electronic band structure. The Fermi surface thus plays an important role establishing the coherent state of the electron-hole pairs. The sharped Drude peak observed in the optical conductivity spectrum has specified that signature. The EI state in this case thus is signified in the BCS type as a superconducting state described by the BCS theory. In the case of $|t^f| = 0.6$, one observes the signature of the optical conductivity spectrum for all values of the electronic hybridization-phonon coupling (see Fig. 6). Indeed, by lowering the mass anisotropy between the conduction and valence electrons, the intermediate Coulomb interaction alone can stabilize the system in the BCS-EI state. Increasing the electronic hybridization-phonon coupling remains the nature of the EI state but reinforces the hybridization between the conduction and valence electrons hence the EI becomes more stable.

To detect dynamical signatures of the excitonic fluctuations before its transition to the EI state in the influence of the mass imbalance and electronic hybridization-phonon coupling, continuously we evaluate the imaginary part of the dynamical excitonic susceptibility function for the Hamiltonian written in Eq. (1). In the randome phase approximation, the dynamical excitonic susceptibility function depending on momentum $\mathbf{q}$ and frequency ω, $\chi(\mathbf{q}, \omega)$, results in

$$\chi(\mathbf{q}, \omega) = -\frac{1}{[\chi^0(\mathbf{q}, \omega)]^{-1} + U - g\Lambda_{\mathbf{q}}}, \tag{17}$$

where $\chi^0(\mathbf{q}, \omega)$ is the bare excitonic susceptibility function, that reads

$$\chi^0(\mathbf{q}, \omega) = \frac{1}{N}\sum_{\mathbf{k}} \frac{f(\bar{\varepsilon}^c_{\mathbf{k}}) - f(\bar{\varepsilon}^f_{\mathbf{k}+\mathbf{q}})}{\omega + i0^+ - \bar{\varepsilon}^f_{\mathbf{k}+\mathbf{q}} + \bar{\varepsilon}^c_{\mathbf{k}}}, \tag{18}$$

and

$$\Lambda_{\mathbf{q}} = \frac{2g\omega_0}{(\omega + i0^+)^2 - \omega_0^2 - \frac{2g^2\omega_0\chi^{0b}(\mathbf{q},\omega)}{1+U\chi^{0b}(\mathbf{q},\omega)}}, \tag{19}$$

with

$$\chi^{0b}(\mathbf{q}, \omega) = \frac{1}{N}\sum_{\mathbf{k}} \frac{f(\bar{\varepsilon}^f_{\mathbf{k}-\mathbf{q}}) - f(\bar{\varepsilon}^c_{\mathbf{k}})}{\omega + i0^+ - \bar{\varepsilon}^c_{\mathbf{k}} + \bar{\varepsilon}^f_{\mathbf{k}-\mathbf{q}}}, \tag{20}$$

where the single particle energies taking into account the Hartree shifts $\bar{\varepsilon}^{c/f}_{\mathbf{k}}$ are given in Eq. (4). With the solutions of the self-consistent equations above, one can simply deliver the

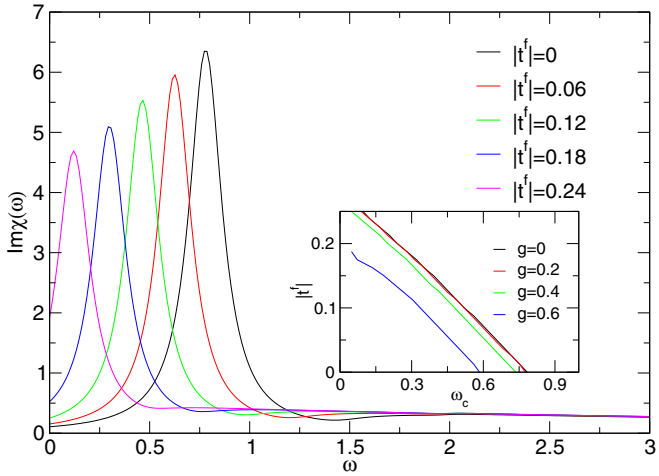

FIG. 7. The imaginary part of the dynamical excitonic susceptibility function at zero momentum, $\mathrm{Im}\chi(\omega)$, for different values of $|t^f|$ at $g = 0.2$ and $U = 3.5$. The inset shows $|t^f|$ as a function of the resonance frequency ω_c for some values of g at $U = 3.5$.

results of $\chi(\mathbf{q}, \omega)$ written in Eq. (17). Moreover, in the direct band-gap situation considering in our present work, the zero momentum excitons are favored [38] and we simplify in our calculation below for the $\mathbf{q} = 0$.

In Fig. 7 we address the imaginary part of the dynamical excitonic susceptibility function at zero momentum, $\mathrm{Im}\chi(\omega)$, for different values of $|t^f|$ at $g = 0.2$ and $U = 3.5$. In this set of parameters, the system settles in the semiconducting state for low $|t^f|$, $|t^f| < 0.25$. For a given low value of $|t^f|$ one always finds the single sharp peak structure in the imaginary part of the dynamical excitonic susceptibility spectra, indicating the preformed coherent bound state of the excitonic fluctuations before the transition to the EI state. The "halo" phase has been mentioned in discussing the stability of the EI in the original EFKM [41]. Increasing $|t^f|$ or suppressing the mass imbalance between the conduction and valence electrons, the peak shifts to the left with lowering energy but its width seems to be unchanged. Varying the mass anisotropy thus does not impact on lifetime of the resonance state; however, its correlation length is raised by lowering the mass imbalance. That signature specifies the tendency to stabilize the EI state by increasing the $|t^f|$ for a given electronic hybridization-phonon coupling (e.g., see the phase diagram in Fig. 4). Suppressing the mass imbalance between the conduction and valence electrons thus plays an important role in establishing and reinforcing the excitonic fluctuations on the semiconductor side. For a given electronic hybridization-phonon coupling, the resonance peak energy ω_c shifts linearly to the left as suppressing the mass anisotropy (see the inset). The inset also shows us that as increasing the electronic hybridization-phonon coupling the linear line moves to the left signifying the reinforcement of the preformed excitonic bound states on the semiconducting side. The results addressed in Fig. 7 have thus specified the significant impacts of the phonon correlation and also the mass imbalance in the stability of the preformed excitonic coherent state or the EI fluctuations even in the semiconducting state.

IV. CONCLUSION

To conclude, in the present work, we have addressed the important impacts of the electron-phonon correlations and the mass imbalance of the electrons and holes on the formation and stability of the excitonic insulator states in semimetal/semiconducting materials. In the framework of the unrestricted Hartree-Fock approach, we have found a set of self-consistent equations determining the excitonic insulator order parameter for the extended Falicov-Kimball model involving the electronic hybridization-phonon coupling. The complex phase diagram of the excitonic insulator states in the influence of the mass imbalance and the electronic hybridization-phonon coupling then has been discussed. For a given intermediate Coulomb interaction, one finds the stability of the excitonic insulator states in case of sufficiently large electronic hybridization-phonon coupling. The condensation window expands if the mass imbalance is suppressed. The influence of the mass imbalance and electron-phonon correlation on the nature of the BCS-BEC crossover of the condensation state is also addressed in the signatures of the optical conductivity. In the features of the dynamical excitonic susceptibility function, the excitonic bound states preformed before the transition to the excitonic insulator state are inspected. That "halo" state in the semiconducting side has been specified by the appearance of a sharp peak in the imaginary part of the dynamical excitonic susceptibility function. By increasing the electronic hybridization-phonon coupling or suppressing the mass imbalance, we find a shift to the lower energy of the peak position indicating the dominance of the preformed bound state. Inspecting the impact of the electronic hybridization-phonon coupling and the mass imbalance in the nature of the excitonic insulator state by taking into account the quantum fluctuations out of the Hartree-Fock approximation would be valuable for our future studies.

ACKNOWLEDGMENT

This research is funded by Hanoi University of Mining and Geology, Vietnam, under Grant No. T23-15.

[1] A. Kavokin, T. C. H. Liew, C. Schneider, P. G. Lagoudakis, S. Klembt, and S. Hoefling, Nat. Rev. Phys. **4**, 435 (2022).
[2] E. C. Regan, D. Wang, E. Y. Paik, Y. Zeng, L. Zhang, J. Zhu, A. H. MacDonald, H. Deng, and F. Wang, Nat. Rev. Mater. **7**, 778 (2022).
[3] N. F. Mott, Philos. Mag. **6**, 287 (1961).
[4] R. Knox, in *Solid State Physics*, edited by F. Seitz and D. Turnbull (Academic Press, New York, 1963), p. 100.
[5] W. Kohn, in *Many Body Physics*, edited by C. de Witt and R. Balian (Gordon & Breach, New York, 1968).
[6] B. Bucher, P. Steiner, and P. Wachter, Phys. Rev. Lett. **67**, 2717 (1991).

[7] P. Wachter, Adv. Mater. Phys. Chem. **08**, 120 (2018).
[8] K. Kim, H. Kim, J. Kim, C. Kwon, J. S. Kim, and B. J. Kim, Nat. Commun. **12**, 1969 (2021).
[9] P. A. Volkov, M. Ye, H. Lohani, I. Feldman, A. Kanigel, and G. Blumberg, npj Quant. Mater. **6**, 52 (2021).
[10] Y.-S. Zhang, J. A. N. Bruin, Y. Matsumoto, M. Isobe, and H. Takagi, Phys. Rev. B **104**, L121201 (2021).
[11] C. Chen, X. Chen, W. Tang, Z. Li, S. Wang, S. Ding, Z. Kang, C. Jozwiak, A. Bostwick, E. Rotenberg *et al.*, Phys. Rev. Res. **5**, 043089 (2023).
[12] B. Zenker, H. Fehske, and H. Beck, Phys. Rev. B **90**, 195118 (2014).
[13] H. Watanabe, K. Seki, and S. Yunoki, Phys. Rev. B **91**, 205135 (2015).
[14] T.-H.-H. Do, D.-H. Bui, and V.-N. Phan, Europhys. Lett. **119**, 47003 (2017).
[15] T.-H.-H. Do, H.-N. Nguyen, and V.-N. Phan, J. Electron. Mater. **48**, 2677 (2019).
[16] T.-H.-H. Do and V.-N. Phan, Phys. Rev. B **107**, 115106 (2023).
[17] L. M. Falicov and J. C. Kimball, Phys. Rev. Lett. **22**, 997 (1969).
[18] V.-N. Phan, K. W. Becker, and H. Fehske, Phys. Rev. B **81**, 205117 (2010).
[19] D. Ihle, M. Pfafferott, E. Burovski, F. X. Bronold, and H. Fehske, Phys. Rev. B **78**, 193103 (2008).
[20] C. D. Batista, Phys. Rev. Lett. **89**, 166403 (2002).
[21] C. D. Batista, J. E. Gubernatis, J. Bonča, and H. Q. Lin, Phys. Rev. Lett. **92**, 187601 (2004).
[22] H. Min, R. Bistritzer, J. J. Su, and A. H. MacDonald, Phys. Rev. B **78**, 121401(R) (2008).
[23] N. V. Phan and H. Fehske, New J. Phys. **14**, 075007 (2012).
[24] A. Perali, D. Neilson, and A. R. Hamilton, Phys. Rev. Lett. **110**, 146803 (2013).
[25] S. Conti, D. Neilson, F. M. Peeters, and A. Perali, Condens. Matter **5**, 22 (2020).
[26] Q.-H. Ninh and V.-N. Phan, Physica Status Solidi B **258**, 2000564 (2021).
[27] A. Kogar, M. S. Rak, S. Vig, A. A. Husain, F. Flicker, Y. I. Joe, L. Venema, G. J. MacDougall, T. C. Chiang, E. Fradkin *et al.*, Science **358**, 1314 (2017).
[28] G. Wang, A. Chernikov, M. M. Glazov, T. F. Heinz, X. Marie, T. Amand, and B. Urbaszek, Rev. Mod. Phys. **90**, 021001 (2018).
[29] A. Georges, G. Kotliar, W. Krauth, and M. J. Rozenberg, Rev. Mod. Phys. **68**, 13 (1996).
[30] G. Czycholl, Phys. Rev. B **59**, 2642 (1999).
[31] P. Farkašovský, Phys. Rev. B **77**, 155130 (2008).
[32] C. Schneider and G. Czycholl, Eur. Phys. J. B **64**, 43 (2008).
[33] T. Soejima, D. E. Parker, N. Bultinck, J. Hauschild, and M. P. Zaletel, Phys. Rev. B **102**, 205111 (2020).
[34] N. Bultinck, E. Khalaf, S. Liu, S. Chatterjee, A. Vishwanath, and M. P. Zaletel, Phys. Rev. X **10**, 031034 (2020).
[35] S. Ejima, T. Kaneko, Y. Ohta, and H. Fehske, Phys. Rev. Lett. **112**, 026401 (2014).
[36] T. Kaneko, S. Ejima, H. Fehske, and Y. Ohta, Phys. Rev. B **88**, 035312 (2013).
[37] V.-N. Phan, K. W. Becker, and H. Fehske, Phys. Rev. B **88**, 205123 (2013).
[38] T.-H.-H. Do and V.-N. Phan, J. Phys.: Condens. Matter **34**, 165602 (2022).
[39] S. Elitzur, Phys. Rev. D **12**, 3978 (1975).
[40] J. K. Freericks and V. Zlatić, Rev. Mod. Phys. **75**, 1333 (2003).
[41] N. V. Phan, H. Fehske, and K. W. Becker, Europhys. Lett. **95**, 17006 (2011).
[42] H. Bruus and K. Flensberg, *Many-Body Quantum Theory in Condensed Matter Physics: An Introduction* (Oxford University Press, New York, 2004).
[43] T.-H.-H. Do, M.-T. Tran, and V.-N. Phan, Phys. Rev. B **106**, 035120 (2022).